

Templated Synthesis of Glycoluril Hexamer and Monofunctionalized Cucurbit[6]uril Derivatives

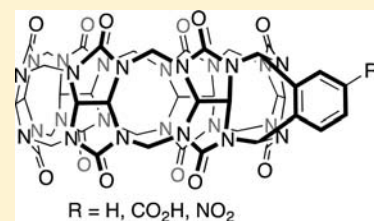
Derick Lucas,[†] Tsuyoshi Minami,[‡] Greg Iannuzzi,[†] Liping Cao,[†] James B. Wittenberg,[†] Pavel Anzenbacher, Jr.,^{*,‡} and Lyle Isaacs^{*,†}

[†]Department of Chemistry and Biochemistry, University of Maryland, College Park, Maryland 20742, United States

[‡]Department of Chemistry and Center for Photochemical Sciences, Bowling Green State University, Bowling Green, Ohio 43403, United States

 Supporting Information

ABSTRACT: We report that the *p*-xylylenediammonium ion (**11**) acts as a template in the cucurbit[*n*]uril forming reaction that biases the reaction toward the production of methylene bridged glycoluril hexamer (**6C**) and bis-nor-seco-CB[10]. Hexamer **6C** is readily available on the gram scale by a one step synthetic procedure that avoids chromatography. Hexamer **6C** undergoes macrocyclization with (substituted) phthalaldehydes **12**, **14**, **15**, and **18**—in 9 M H₂SO₄ or concd HCl at room temperature to deliver monofunctionalized CB[6] derivatives **13**, **16**, **17**, and **19**—that are poised for further functionalization reactions. The kinetics of the macrocyclization reaction between hexamer and formaldehyde or phthalaldehyde depends on the presence and identity of ammonium ions as templates. *p*-Xylylenediammonium ion (**11**) which barely fits inside CB[6] sized cavities acts as a *negative template* which slows down transformation of **6C** and paraformaldehyde into CB[6]. In contrast, **11** and hexanediammonium ion (**20**) act as a *positive template* that promotes the macrocyclization reaction between **6C** and **12** to deliver (\pm)-**21** as a key intermediate along the mechanistic pathway to CB[6] derivatives. Naphthalene-CB[6] derivative **19** which contains both fluorophore and ureidyl C=O metal-ion (e.g., Eu³⁺) binding sites forms the basis for a fluorescence turn-on assay for suitable ammonium ions (e.g., hexanediammonium ion and histamine).



INTRODUCTION

The cucurbit[*n*]uril (CB[*n*]; *n* = 5, 6, 7, 8, 10) family of molecular container compounds are prepared by the condensation reaction of glycoluril (**1**) and formaldehyde under strongly acidic conditions (Chart 1).^{1,2} Interest in CB[*n*] molecular containers³ has surged in recent years, in large part due to the high affinity (K_a up to 10^{15} M^{-1}) and highly selective (K_{rel} up to 10^8 for closely related guests) binding processes that occur inside the CB[*n*] cavity.^{4–7} These large differences in binding free energy amount to a potent driving force that can be used to drive switching processes in biological and technological applications. For example, CB[*n*]·guest complexes have been used in applications ranging from stimuli responsive molecular machines,⁸ supramolecular polymers,⁹ sensing ensembles,^{10,11} and in biomimetic systems.^{12–14} Still other application areas include drug delivery,^{15–17} gas purification,¹⁸ and supramolecular catalysis.¹⁹ Despite the wide range of applications to which the parent unfunctionalized CB[*n*] compounds may be applied, there is real need for versatile synthetic methods for the preparation of CB[*n*] derivatives that contain reactive functional groups that are amenable to further functionalization reactions for incorporation into more complex systems. To date, the most versatile method for the functionalization of CB[*n*] compounds is the (per)hydroxylation of CB[*n*] developed by the Kim group,²⁰ who have used the (per)hydroxylated CB[*n*] compounds for several applications including membrane protein fishing and stimuli responsive

polymer nanocapsules for drug delivery.^{16,21} Despite these advances, the preparation of monofunctionalized CB[*n*] compounds containing reactive functional groups remains unknown.

For many years, our group has been interested in understanding the mechanism of CB[*n*] formation (Scheme 1) as a means to prepare new CB[*n*]-type receptors with the goal of endowing the synthesized CB[*n*] compounds with exciting new functions.^{14,22} This line of inquiry has led us to prepare CB[*n*] analogues,²³ inverted CB[*n*],²⁴ and nor-seco-CB[*n*] containers^{13,25,26} (Chart 1) which were demonstrated to function in applications including UV/vis and fluorescence sensing, chiral recognition, size-dependent homotropic allostery, and foldamer reconfiguration. In the course of these studies, we have garnered mechanistic information that suggested to us that templated synthesis of CB[*n*]-type compounds would be possible. For example, we established the presence of an equilibrium between S-shaped and C-shaped glycoluril oligomers (e.g., **2C**–**8C**)²⁷ that greatly favors the C-shaped form required for the formation of CB[*n*]-type receptors.²⁸ We also showed that the macrocyclization reaction to give CB[*n*]-type receptors occurs by a combination of chain growth and step growth processes.^{27,29,30} Previously, Day and co-workers studied the influence of potential templating compounds (e.g., metal ions or ammonium ions) on the product distribution of the CB[*n*]

Received: August 31, 2011

Published: October 04, 2011

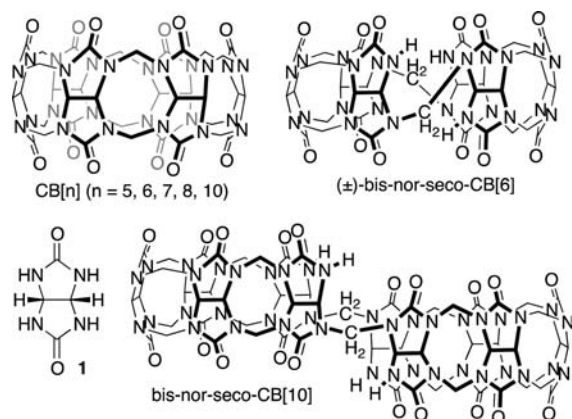
forming reaction.³¹ Although the presence of templates does effect the ratio of CB[n] formed, the effects are generally modest and the underlying mechanistic reasons for those effects remain unclear. In this paper, we explore the templated synthesis of methylene bridged glycoluril hexamer (6C), the transformation of 6C into monofunctionalized CB[6] derivatives by reaction with (substituted) phthalaldehydes in the presence of templates, and demonstrate unique sensing abilities of a CB[6] derivative covalently functionalized with a naphthalene fluorophore.

RESULTS AND DISCUSSION

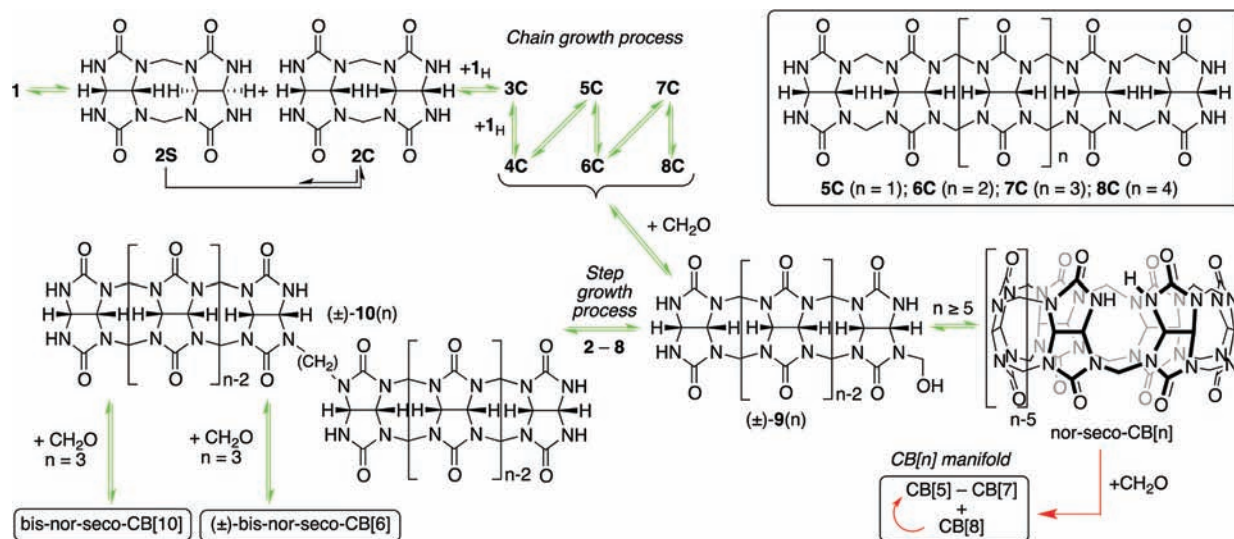
This results and discussion section is subdivided into several subsections detailing the template synthesis of glycoluril hexamer 6C and bis-ns-CB[10], the transformation of 6C into CB[6] derivatives, exploration of the basic recognition properties of these CB[6] derivatives, and their use in creating a turn-on fluorescence sensor for biologically important histamine.

Mechanism of CB[n] Formation. First, we review the state-of-the-art understanding of the mechanism of CB[n] formation (Scheme 1) which is required to understand our hypothesis that

Chart 1. Structures of Glycoluril (1), CB[n], (±)-Bis-nor-seco-CB[6], and Bis-nor-seco-CB[10]



Scheme 1. Mechanism of CB[n] Formation^a



^a Color code: reversible equilibria, green arrows; irreversible reactions, red arrows.

templated formation of CB[n]-type receptors will be possible when the reactions are conducted with fewer than 2 equiv of formaldehyde. In brief, the condensation of two molecules of glycoluril (1) with two molecules of formaldehyde delivers a mixture of C-shaped 2C and its S-shaped diastereomer 2S. Previous model system studies have shown that the C-shaped diastereomer is more stable than the S-shaped form by >1.55 kcal mol⁻¹, so isomerization to the more stable 2C occurs readily under the reaction conditions.²⁹ Dimer 2C can undergo chain growth by the stepwise addition of glycoluril (1) to deliver trimer–octamer (3C–8C); at each step along the way, isomerization from the less stable S-shaped to the more stable C-shaped forms occur. At this stage, two mechanistic pathways may occur. In the first pathway, two molecules of oligomer (e.g., pentamer 5C) may condense with two molecules of formaldehyde via intermediates (±)-9 (n = 5) and (±)-10 (n = 5) which leads to bis-nor-seco-CB[10] by a step growth process. Similar step growth processes lead to (±)-bis-nor-seco-CB[6] and an acyclic glycoluril decamer that we have studied previously.^{13,26} A second pathway involves the condensation of 6C with formaldehyde to initially deliver (±)-9 (n = 6) followed by macrocyclization to give nor-seco-CB[6]. On the basis of the results of model system studies and product resubmission experiments, we depict all of these fundamental steps with reversible equilibrium arrows.^{27,32} Finally, the reaction of nor-seco-CB[n] with formaldehyde delivers CB[n]. Within the CB[n] product manifold, resubmission experiments conducted by Day establish that CB[8] undergoes contraction to the smaller CB[n] (n = 5, 6, 7) but that CB[5], CB[6], and CB[7] are stable to the reaction conditions.² Therefore, CB[5]–CB[7] are kinetic traps in the CB[n] forming reaction; the relative thermodynamic stability of CB[5], CB[6], and CB[7] have not been established experimentally. This result implies that the final ring closing transformation of nor-seco-CB[n] to CB[n] is irreversible under the reaction conditions. On the basis of this analysis, it is perhaps unsurprising that previous attempts to use ammonium ions that are good guests for CB[n] as thermodynamic templates have not been particularly successful. The key hypothesis explored in this paper is whether substituted ammonium ions (e.g., p-xylylenediammonium ion 11) are

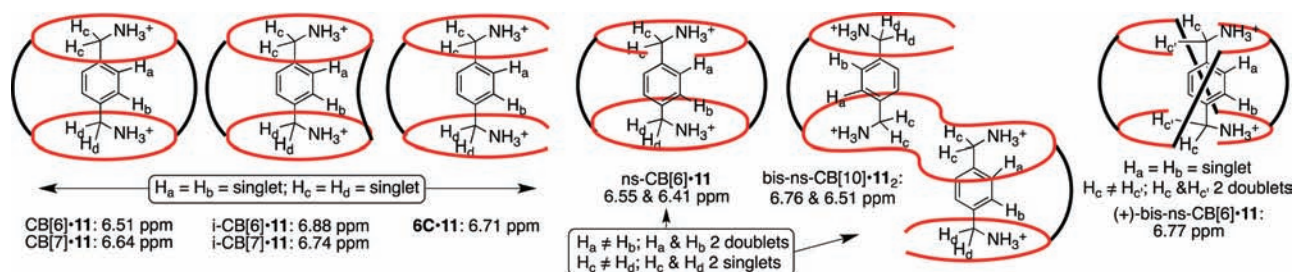


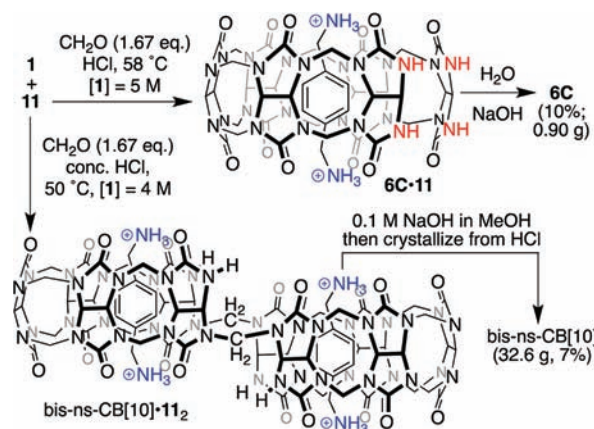
Figure 1. Illustration of the use of **11** as a probe of $\text{CB}[n]$ reaction mixtures by ^1H NMR spectroscopy.

suitable templates for nor-seco- $\text{CB}[n]$ forming reactions conducted between 1 equiv of glycoluril and less than 2 equiv of formaldehyde. Under these formaldehyde deficient reaction conditions, irreversible cyclization to $\text{CB}[n]$ is slowed down²⁷ allowing thermodynamic effects to become enhanced.

Classification of Templates. Classification of the different types of template effects that may occur in covalent bond forming reactions has been beautifully reviewed by Anderson and Sanders and is therefore only briefly described here.³³ Template molecules promote the formation of a specific product by either kinetic or thermodynamic means. Thermodynamic templates enhance the yield of reactions under thermodynamic control by stabilizing one product at the expense of others. Kinetic templates influence the yield of a particular product by changing the various transition state energies and therefore the rate of product formation. Kinetic templates may be further classified as positive or negative based on whether they speed up or slow down the rate of formation of a particular product, respectively. Finally, because kinetic templates, which influence transition state energies, typically bind to reaction intermediates or products, they commonly also exert thermodynamic influences on the reaction.

Templated Synthesis of Hexamer **6C and Bis-nor-seco- $\text{CB}[10]$.** *Selection of Para-xylylenediammonium Ion as Template and ^1H NMR Probe Guest.* On the basis of the hypothesis described above, we decided to conduct reactions between 1 equiv of glycoluril (**1**) and less than 2 equiv of formaldehyde in the presence of an ammonium ion as template. As the template ammonium ion we selected *p*-xylylenediammonium ion (**11**) for several reasons (Figure 1). First, **11** is known to form well-defined host-guest complexes with $\text{CB}[6]$, $\text{CB}[7]$, $\text{CB}[8]$, *i*- $\text{CB}[6]$, *i*- $\text{CB}[7]$, **6C**, bis-nor-seco- $\text{CB}[10]$, (\pm)-bis-nor-seco- $\text{CB}[6]$, and nor-seco- $\text{CB}[6]$ which means that **11** could conceivably act as a stabilizing template for many different $\text{CB}[n]$ -type receptors. Second, because the kinetics of exchange for complexes of **11** with each of these containers is slow on the NMR time scale, each different container·**11** complex gives a diagnostic pattern of resonances in the ^1H NMR spectrum (Figure 1). For example, for highly symmetric hosts ($\text{CB}[6]$, $\text{CB}[7]$, *i*- $\text{CB}[6]$, *i*- $\text{CB}[7]$, and **6C**), the ^1H NMR resonance for the Ar-H atoms of **11** appears as a sharp singlet in the relatively open 6–7 ppm region of the ^1H NMR spectrum (Figure 1 and Supporting Information). Conversely, for less symmetric bis-nor-seco- $\text{CB}[10]$ ·**11**₂ and nor-seco- $\text{CB}[6]$ ·**11** complexes, the Ar-H (H_a and H_b) atoms are nonequivalent and appear as a pair of doublets. Finally, for (\pm)-bis-ns- $\text{CB}[6]$ ·**11**, the Ar-H (H_a and H_b) atoms are equivalent and appear as a singlet but the CH_2 -groups of guest **11** are diastereotopic (H_c and H_d) and appear as a pair of doublets in the upfield region of the spectrum. Third, we find that using **11** as guest tends to result in good dispersion of the host resonances for the less symmetrical host·**11** complexes. For these reasons, it was

Scheme 2. Templated Synthesis of **6C** and Bis-nor-seco- $\text{CB}[10]$



particularly efficacious to use **11** as template and simultaneously as an in situ probe for analysis of the content of $\text{CB}[n]$ reaction mixtures.

*Discovery of Templated Synthesis of Hexamer **6C**.* After much experimentation, we discovered that heating a mixture of **1** (7.1 g, 1 equiv, 5 M), paraformaldehyde (1.67 equiv), and **11** (0.1 equiv) in concentrated HCl at 58 °C for 3–5 days delivers a thick off-white precipitate that can be isolated by centrifugation.³⁴ Analysis of the ^1H NMR spectrum of the precipitate indicates that it contains mainly (\approx 89% purity) the **6C**·**11** complex (Scheme 2). We also analyzed the content of the supernatant by ^1H NMR. The supernatant contains 11% **6C**, 10% bis-ns- $\text{CB}[10]$, 5% nor-seco- $\text{CB}[6]$, 5% $\text{CB}[6]$, along with unidentified species. To obtain free **6C**, we dissolved the crude solid in water, centrifuged away insoluble materials, and then added 5 M aq NaOH which resulted in the precipitation of **6C**. Hexamer **6C** is obtained as a white powder (0.901 g, 10% yield). Our hypothesis is that the presence of **11** as template served at least two purposes: (1) to bind to **6C** and therefore thermodynamically stabilize it, and (2) to cause precipitation which also thermodynamically stabilizes **6C** toward further transformation. In an attempt to further optimize this reaction, we changed some key variables (e.g., temperature, acid concentration, equivalents of **11**, equivalents of formaldehyde) but were unable to further improve the process.

Templated Synthesis of Bis-nor-seco- $\text{CB}[10]$. Previously, we have reported that the reaction of **1** (1.42 g, 1 equiv, 2.5 M) and paraformaldehyde (1.67 equiv) in concd HCl at 50 °C delivers bis-nor-seco- $\text{CB}[10]$ as an insoluble precipitate (0.238 g, 15%). We found that this reaction is very sensitive to many variables

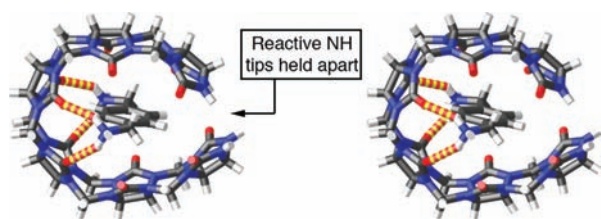


Figure 2. Stereoview of an MMFF minimized model of the $6C \cdot 11$ complex.

including the initial mixing of the solid reagents with the HCl solvent, the nature of the reaction vessel (20 mL scintillation vial preferred), and the nature of the vessel closure (14/20 Suba-Seal attached with copper wire preferred).³⁵ Given the high sensitivity of this reaction, it is perhaps unsurprising that we have been unable to scale-up this reaction to the 10 or 100 g levels; reactions on this scale typically deliver large amounts of CB[6] as product. Since the CB[*n*] forming reaction is a cyclo-oligomerization reaction²⁷ whose fundamental condensation steps respond to changes in concentration over the millimolar to molar range,³² we reasoned that it would be worthwhile to perform the **11** templated reaction at higher concentrations of **1**. For example, when the reaction is conducted using 400 g of **1** with $[1] = 4$ M, the reaction mixture remains homogeneous and ¹H NMR analysis of the crude reaction mixture reveals the presence of bis-ns-CB[10] (11%), **6C** (6%), ns-CB[6] (5%), and CB[6] (13%). The more soluble compounds **6C**, CB[6], and ns-CB[6] were removed by washing with H₂O.³⁶ Decomplexation of bis-nor-seco-CB[10]·**11**₂ by washing with 0.1 M NaOH in MeOH followed by recrystallization from HCl delivered bis-ns-CB[10] (32.6 g, 7% yield). The observation of the enhanced formation of bis-nor-seco-CB[10] (derived from two units of pentamer **5C**) at lower concentrations and hexamer **6C** at higher concentrations of **1** is consistent with our description of the mechanism of CB[*n*] formation as a copolymerization process between **1** and formaldehyde which is expected to deliver longer oligomers at higher concentrations according to Le Chatelier's principle.

The Role of Template 11 in CB[*n*] Forming Reactions. There are many possible roles for template **11** in these reactions (e.g., thermodynamic, kinetic, positive, negative). First, it is known from the literature that **11** binds to **5C** ($K_a = 1.2 \times 10^6$ M⁻¹) and **6C** ($K_a = 2.2 \times 10^7$ M⁻¹) substantially stronger than it does to either CB[6] ($K_a = 550$ M⁻¹) or a tetramethyl derivative of **4C** ($K_a = 5.6 \times 10^3$ M⁻¹).³⁰ This information suggests that the formation of the $6C \cdot 11$ and bis-nor-seco-CB[10]·**11**₂ complexes thermodynamically stabilize these oligomers. Second, the precipitation of the $6C \cdot 11$ complex suggests that complexation of **6C** with **11** changes the maximal solubility of the $6C \cdot 11$ complex (relative to **6C**) which in turn results in precipitation when that solubility limit is exceeded. Third, Figure 2 shows an MMFF minimized model of the $6C \cdot 11$ complex. An examination of this complex shows that the presence of guest **11** enforces a geometry in which the reactive NH tips of **6C** are held apart from each other.³⁷ This geometrical feature might kinetically disfavor transformation of $6C \cdot 11$ into CB[6]·**11**.

Given access to gram-scale quantities of **6C**, we decided to study the kinetics of the transformation of **6C** and paraformaldehyde into CB[6] in the absence or presence of **11** as template as a means to assess the importance of kinetic stabilization of the $6C \cdot 11$ complex on the reaction. We conducted the reactions in

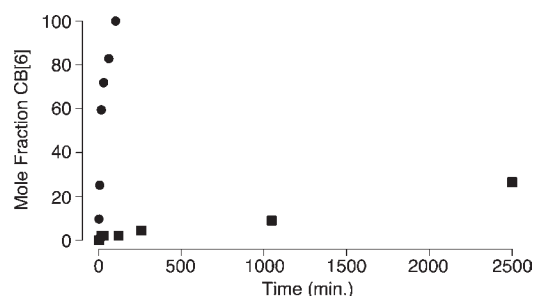


Figure 3. Plot of mole fraction of CB[6] versus time for reactions between **6C** and paraformaldehyde in the absence (●) or presence (■) of **11** as template.

concd HCl at room temperature with $[6C] = 200$ mM. Figure 3 shows plots of the mole fraction of CB[6] determined by integration of the ¹H NMR spectra recorded versus time. After less than 2 h, the untemplated reaction is complete, whereas in the presence of **11** as template, the reaction is only 2% complete. Clearly, the presence of **11** as template substantially slows down the macrocyclization reaction between **6C** and formaldehyde to deliver CB[6] as product.

Accordingly, it appears that **11** as template serves several roles in influencing the outcome of CB[*n*] forming reactions. These roles include differential thermodynamic stabilization due to complex formation, controlling the solubility of various components of the reaction mixture through complexation, and finally in influencing the kinetics of the macrocyclization step of the CB[*n*] forming reaction. Because of the complexity of the analysis of such reaction mixtures using templates other than **11**, we have not yet been able to expand our study to the full range of potential templates.

Transformation of 6C into Monofunctionalized CB[6] Derivatives. Previously, we have studied the reaction between 2 equiv of *N,N'*-dimethylglycoluril with *o*-phthalaldehyde (**12**) under acidic conditions and observed the dominant formation of S-shaped products.³² However, we reasoned that the reaction between **6C** and **12** might be successful because **6C** is preorganized to form the C-shaped macrocyclic product (Scheme 3). In the event, we allowed **6C** (1 g) to react with **12** in 9 M H₂SO₄ at room temperature for 36 h. Purification of the crude reaction mixture was easily achieved by a combination of precipitation and washing steps to deliver CB[6] derivative **13** in 72% yield (792 mg). Compound **13** is C_{2v}-symmetric and that is reflected in the simplicity of its ¹H NMR spectrum recorded as its **13**·**11** complex (Figure 4a). The most diagnostic resonances in the ¹H NMR spectra are those for host protons H_n (6.89 ppm) as well as H_o and H_p (4.93 and 5.12 ppm) which are upfield shifted due to their proximity to the fused aromatic *o*-xylylene ring. Similar reactions were conducted between **6C** and carboxylic acid or nitro-substituted phthalaldehydes **14**³⁸ and **15**³⁹ which delivered monofunctionalized CB[6] derivatives **16** and **17** in 56% (641 mg) and 58% (65 mg), respectively.⁴⁰ Figure 4c,d shows their ¹H NMR spectra recorded as their complexes with **11** which reflects the lower C_s-symmetry of these CB[6] derivatives. Finally, we conducted the reaction between **6C** (1 g) and 2,3-naphthalenedialdehyde **18**⁴¹ in concd HCl at room temperature and obtained **19** as a precipitate. Simple washing with MeOH delivered **19** in pure form (83%, 0.951 g). Unfortunately, we have not been able to obtain crystals of **13**, **16**, **17**, or **19** that are suitable for X-ray crystallographic structure determination.

Scheme 3. Synthesis of CB[6] Derivatives 13, 16, 17, and 19

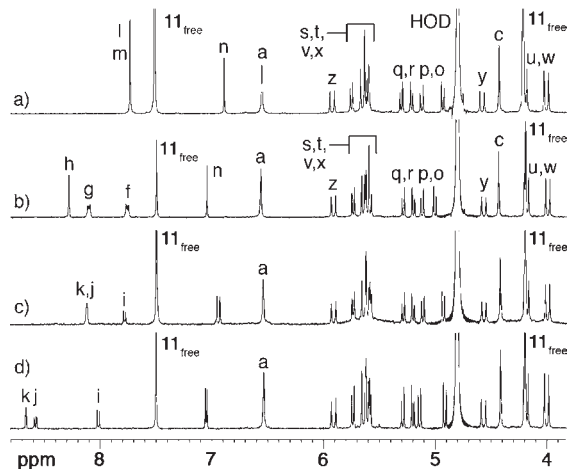
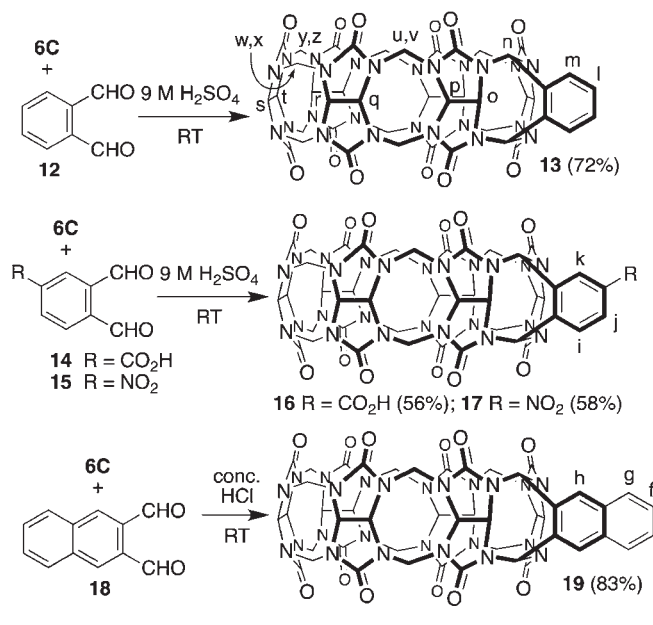


Figure 4. ¹H NMR spectra recorded (400 MHz, D₂O, RT) for: (a) 13·11, (b) 19·11, (c) 16·11, and (d) 17·11. Only partial assignments are given in panels c and d because the lower symmetry of 16 and 17 complicates the assignments.

To provide some structural information, we minimized the structure of 13 by MMFF calculations (Figure 5). As is readily apparent, the fusion of the *o*-xylylene ring to the methylene bridges of the CB[6] skeleton results in an overall ellipsoidal deformation of the cavity along the plane defined by the *o*-xylylene ring. Similar deformations have been observed for CB[6] derivatives prepared from substituted glycolurils⁴² and for certain CB[6]·guest complexes.⁴³ Since the main reason to prepare CB[6] derivatives is to use their host·guest binding properties to enable advanced applications, it is critical that the CB[6] derivatives maintain the high affinity and high selectivity binding interactions typical of the CB[*n*] family. Given the ellipsoidal deformation described above, we decided that it was necessary to experimentally determine the binding constant of these new CB[6] derivatives toward common guests.

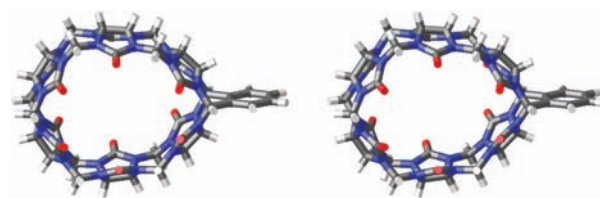


Figure 5. Stereoview of the MMFF minimized structure of 13.

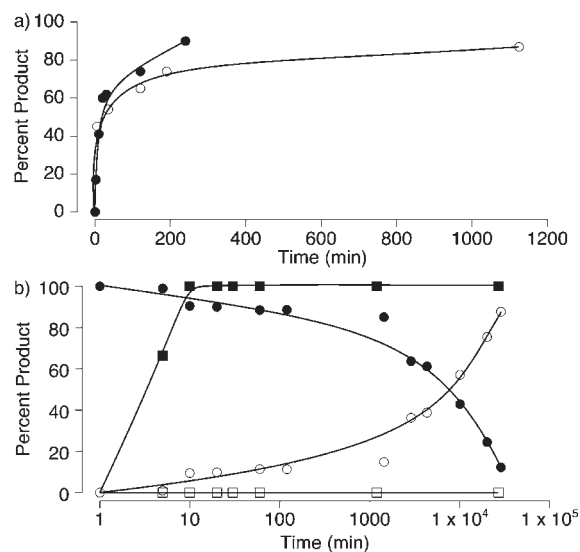


Figure 6. Plot of percent product 13 and (±)-21 versus time for the reaction of 6C with 12 (9 M H₂SO₄, RT): (a) percent 13 in the absence of template (●) or with NH₄Cl as template (○), and (b) in the presence of 20 as template (● = percent (±)-21; ○ = percent 13) or 11 as template (■ = percent (±)-21; □ = percent 13).

Template Effects Also Operate During the Reaction between 6C and 12. The observation of intermediates by ¹H NMR during the reactions between 6C and 12 shown in Scheme 3 suggested to us that it might be possible to observe the influence of templates on the reaction between 6C and 12. First, we monitored the kinetics of the reaction between 6C and 12 in the absence of any template (Figure 6a, ●) and observed that the reaction delivered 13 over 240 min. Similarly, when NH₄⁺, which can bind to the ureidyl C=O portals but not the hydrophobic cavities of CB[6] compounds, is used as template, we observe comparable reaction kinetics as the untemplated reaction. The situation is very different when larger diammonium ions 20 and 11 are used as templates. For example, when 6C reacts with 12 in the presence of 20 as template (9 M H₂SO₄, RT), the reaction very rapidly (<1 min) gives an intermediate ((±)-21) which very slowly transforms (over several weeks) into 13·20 (Figure 6b, ● = (±)-21; ○ = 13·20). However, when the reaction between 6C and 12 was conducted (9 M H₂SO₄, RT) in the presence of 11 as template (Figure 6b, ■ = (±)-21; □ = 13·11), the reaction again rapidly delivers intermediate ((±)-21) that is kinetically stable over the course of several weeks. Attempts to stop either of these templated reactions at the intermediate stage, remove template, and purify by Dowex ion exchange chromatography were uniformly unsuccessful for the reason detailed below. Fortunately, a sample containing predominantly (±)-21 could be obtained when the reaction between 6C and 12 was conducted in CF₃CO₂H as

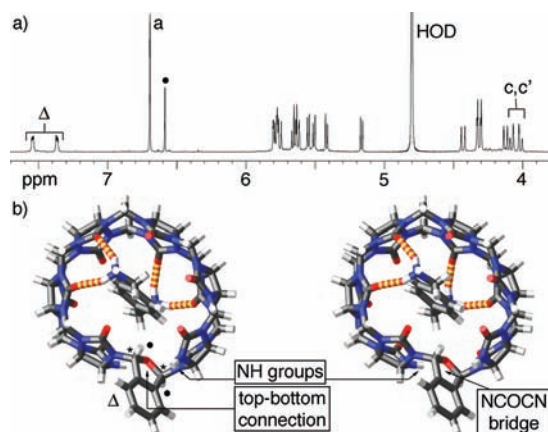
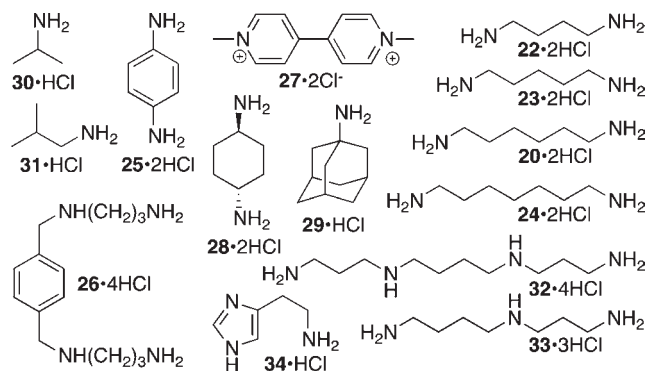


Figure 7. (a) ^1H NMR spectrum recorded for $(\pm)\text{-}21 \cdot 11$ (600 MHz, D_2O , RT). (b) MMFF minimized models of one diastereomer of $(\pm)\text{-}21 \cdot 11$. Asterisk (*) = stereogenic center.

solvent. We characterized $(\pm)\text{-}21$ as its $(\pm)\text{-}21 \cdot 11$ complex. The electrospray ionization mass spectrum showed a peak at $m/z = 613.15$ amu which can be rationalized as arising from the reaction between **6C** (972 amu), **12** (134 amu), and $\mathbf{11}^{2+}$ (138 amu) with expulsion of one molecule of H_2O . The 600 MHz ^1H NMR spectrum of the complex (Figure 7a) provided key clues which allowed us to determine the structure as $(\pm)\text{-}21 \cdot 11$ (Figure 7b). For example, the singlet at 6.59 ppm corresponds to the four symmetry equivalent Ar–H protons (H_a) of guest **11** which establishes that the two ureidyl C=O portals of $(\pm)\text{-}21$ are symmetry equivalent (see Figure 1, $\text{CB}[n]$, $i\text{-CB}[n]$, **6C**, $(\pm)\text{-bis-nor-seco-CB}[6]$). The upfield region of the ^1H NMR spectrum shows a pair of coupled doublets at 4.08 and 4.01 ppm which correspond to the diastereotopic CH_2 -group (H_c , H_c') of guest **11** which indicates that $(\pm)\text{-}21$ is chiral and racemic (see Figure 1, $(\pm)\text{-bis-nor-seco-CB}[6]$). On the basis of the combined inference of the ESI–MS and diagnostic ^1H NMR resonances, we formulate the structure of $(\pm)\text{-}21 \cdot 11$ as shown in Figure 7b. This structure features a top-bottom connection between the two ends of the hexamer unit of $(\pm)\text{-}21$ enforced by an NCOCN-bridge⁴⁴ which contains two stereogenic centers.⁴⁵ The availability of free $(\pm)\text{-}21$ allowed us to understand the difficulties that we encountered during the attempted purification of $(\pm)\text{-}21$ during Dowex ion exchange chromatography. When $(\pm)\text{-}21$ was dissolved in H_2O , we observed hydrolysis of the NCOCN-bridge over the course of 4 days to deliver starting material **6C** (Supporting Information, Figure S14).

The observation of $(\pm)\text{-}21 \cdot 11$ as the sole product in the reaction between **6C** and **12** in the presence of **11** is significant for several reasons. First, it represents the first clear-cut example of a high fidelity template effect operating in $\text{CB}[n]$ chemistry.⁴⁶ We believe that the reaction stops at the stage of $(\pm)\text{-}21 \cdot 11$ because this larger cavity is better able to accommodate guest **11** whose affinity toward $\text{CB}[6]$ sized cavities is rather weak. Second, the observed hydrolytic lability of $(\pm)\text{-}21$ provides further evidence of the reversibility of the macrocyclization upon which the success of this thermodynamic template effect is based. Third, the observation of $(\pm)\text{-}21 \cdot 20$ as an intermediate along the pathway to **13**·**20** suggests that size of the guest (e.g., differential affinity toward $(\pm)\text{-}21$ and **13**) might be used in related reactions to template the formation of other, more spacious $\text{CB}[n]$ -type containers.

Chart 2. Chemical Structure of Guests Used in This Study



CB[6] Derivatives Are Capable of Self-Association. Before undertaking the study of any new host system, it is wise to perform ^1H NMR dilution experiments to exclude the possibility of self-association interfering with the host–guest complexation events. We found that diluting a sample of **13** (20 mM NaCO_2CD_3 buffer, pD 4.74) from 2 mM down to 0.06 mM results in a downfield shift of H_l and H_m , and an upfield shift for H_o (Supporting Information). These shifts are consistent with self-association by insertion of the *o*-xylylene ring of **13** into the cavity of another molecule of **13** which positions H_l and H_m in the cavity of the other molecule of **13** and H_o at the deshielding ureidyl C=O portal. We fitted the data to a 2-fold self-association model and obtain $K_{\text{self}} = 1.2 \pm 0.1 \times 10^3 \text{ M}^{-1}$ (Supporting Information). Similar dilution experiments performed with **16**, **17**, and **19** did not reveal any changes in chemical shift which indicates that they do not undergo self-association processes (Supporting Information). Even though **19** does not self-associate, it does form a complex with $\text{CB}[7]$, namely, $\text{CB}[7] \cdot 19$, whose ^1H NMR resonances change little down to 100 μM (Supporting Information). The upfield shifts observed for the naphthalene ring of **19** indicates it is immersed in the cavity of $\text{CB}[7]$. These results highlight the potential of $\text{CB}[6]$ derivatives to undergo complexation with themselves or other species and suggests that care must be taken in designing $\text{CB}[6]$ derivatives for use in advanced applications.

Host-Guest Complexes and Determination of Binding Constants. Given the observed self-association of **13** and the top-bottom dissymmetry of **16** and **17**, we decided to focus our efforts on elucidating the host–guest recognition properties of **19**. Chart 2 shows the structures of guests **20** and **22–34** that were studied. Initially, we measured the ^1H NMR spectra for 1:1 and 1:2 (host/guest) mixtures of host **19** and guests **11**, **20**, and **22–34** (Supporting Information). As expected, the majority of these guests formed **19**·guest inclusion complexes that display slow kinetics of exchange on the ^1H NMR time scale; guests **27**, **30**, and **34** show fast kinetics of exchange. Just like $\text{CB}[6]$, **19** does not form an inclusion complex with adamantane amine **29**. Unlike $\text{CB}[6]$, **19** forms the **19**·**27** inclusion complex which suggests that the observed ellipsoidal deformation (Figure 5) of **19** allows it to bind wider guests like **27**. Figure 8a–d shows the ^1H NMR spectra recorded for **20**, **19**·**20**, **26**, and **19**·**26**. The observed upfield shifts of the hexylene and *p*-xylylene regions of guests **20** and **26** confirm their inclusion inside the cavity of **19** as expected. Interestingly, all three CH_2 -groups of the $^+\text{H}_2\text{N}(\text{CH}_2)_3\text{NH}_3^+$ arms of **26** shift downfield in the **19**·**26** complex which confirms that these groups are in the deshielding region

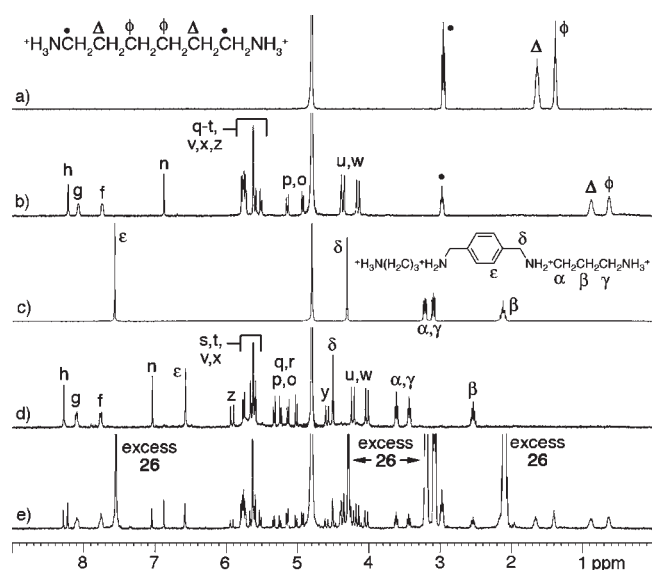


Figure 8. ^1H NMR spectra recorded (400 MHz, 20 mM NaO_2CCD_3 buffered D_2O , pD 4.74, RT) for: (a) **20**, (b) **19**·**20**, (c) **26**, (d) **19**·**26**, and (e) a mixture of **19** (0.5 mM), **20** (0.5 mM), and **26** (5.0 mM).

nearly the ureidyl $\text{C}=\text{O}$ portals of **19**. Overall, the recognition properties of **19** are qualitatively quite similar to those known for $\text{CB}[6]$.

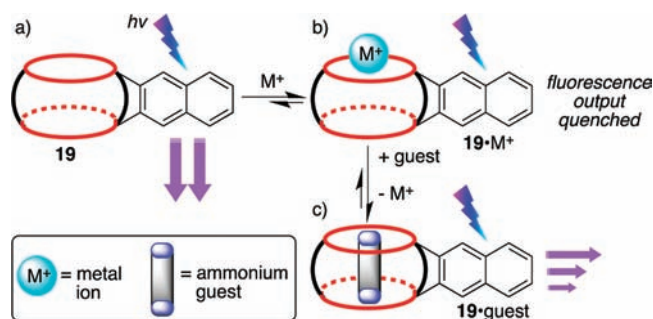
Next, we decided to quantify the **19**·guest binding constants to ascertain whether the ellipsoidal deformation induced by the *o*-xylylene ring (Figure 5) significantly influences values of K_a . First, we measured the value of K_a of **19** toward **30**, which undergoes fast kinetics of exchange on the NMR time scale, by a standard NMR titration in which the concentration of guest **30** was fixed (0.125 mM) and the concentration of **19** was changed (0–1.83 mM) (Supporting Information, Figure S51). Figure S52 shows a plot of the chemical shift of the CH_3 -groups of **30** as a function of $[\mathbf{19}]$ and the nonlinear least-squares fitting to a 1:1 binding model (Table 1, $K_a = 852 \pm 114 \text{ M}^{-1}$). Subsequently, we used the ^1H NMR competition methodology, involving competition of an excess of a mixture of two guests for a limiting amount of **19**, originally developed by Mock⁴ and used extensively by our group^{5,30} to determine K_a values for **19**·guest complexes of increasing stability in a stepwise manner. For example, Figure 8e shows the ^1H NMR spectra used to calculate the relative K_{rel} values for the competition between **19** (0.5 mM), **20** (0.5 mM), and **26** (5.0 mM); we use the integrals for H_n (**19**·**20**, 6.88 ppm; and **19**·**26**, 7.05 ppm) for this purpose. Table 1 reports the values of K_a obtained for nine **19**·guest complexes obtained similarly. The measured values of K_a range from $\approx 10^3 \text{ M}^{-1}$ up to 10^8 M^{-1} in 20 mM NaOAc buffered D_2O at pD 4.74. Table 1 also presents the values of K_a measured previously by Mock and co-workers in 1:1 $\text{HCO}_2\text{H}/\text{H}_2\text{O}$ toward many of these guests. As expected, the values of K_a measured for **19** are larger (up to 50-fold) than the corresponding values measured for $\text{CB}[6]$ because of the effect of the more strongly competitive (1:1 $\text{HCO}_2\text{H}/\text{H}_2\text{O}$) solvent. Similar to $\text{CB}[6]$, **19** exhibits a length dependent selectivity toward alkanediammonium ions **20** and **22**–**24** with highest affinity toward pentane and hexanediammonium ions **23** and **20**.⁴ Tetracationic spermine **34**, which is an outstanding guest for $\text{CB}[6]$,¹⁷ binds very tightly to **19** ($K_a = 1.0 \pm 0.2 \times 10^8 \text{ M}^{-1}$) which will enable the use of derivatives of **19** in a variety of

Table 1. Binding Constants (K_a, M^{-1}) Measured for the Host–Guest Complexes of **19** and Compared to Literature Values for $\text{CB}[6]$ ^a

guest	host 19	$\text{CB}[6]$ ^b
11	$2.7 \pm 0.5 \times 10^3$	550 ± 30^c
22	$4.9 \pm 1.2 \times 10^5$	1.5×10^5
23	$5.7 \pm 1.4 \times 10^6$	2.4×10^6
20	$1.4 \pm 0.3 \times 10^7$	2.8×10^6
24	$2.6 \pm 1.4 \times 10^6$	4.3×10^4
26	$4.7 \pm 1.0 \times 10^5$	n.d. ^d
30	852 ± 114	n.d. ^d
31	$3.0 \pm 0.6 \times 10^4$	2.1×10^4
32	$1.0 \pm 0.2 \times 10^8$	1.3×10^7

^a Conditions: 20 mM NaO_2CCD_3 buffer, D_2O , pD 4.74, RT. ^b Taken from Mock and Shih.⁴ ^c Taken from Isaacs and co-workers.⁵ ^d n.d. = not determined.

Scheme 4. Concept of Fluorescence Assay Based on Fluorescent $\text{CB}[6]$ -Derivative **19**^a



^a (a) Host **19** is excited by UV light and emits fluorescence in response; (b) in the presence of a quenching metal ion, the fluorescence is quenched due to an intra-complex resonance energy transfer from naphthalene to metal; (c) the addition of a guest leads to displacement of the quenching metal ion.

application areas. Overall, the recognition properties of **19** closely parallels those known for unsubstituted $\text{CB}[6]$.

Host 19 Functions as a Turn-On Fluorescence Sensor for Amines. $\text{CB}[n]$ containers have been used previously to construct a variety of sensing ensembles, most notably those prepared by Urbach and Nau that are used to sense the presence of peptides and even proteins.^{11,47} All these assays are based on the indicator displacement assay⁴⁸ in which guest competes with chromophore or fluorophore for binding inside the $\text{CB}[n]$ cavity. We envisioned that $\text{CB}[6]$ derivative **19** with its covalently attached 2,3-dialkyl naphthalene fluorophore, its metal binding⁴⁹ ureidyl $\text{C}=\text{O}$ portals, and its hydrophobic cavity⁷ could form the basis for a new type of fluorescence based $\text{CB}[n]$ sensing system. The concept is illustrated in Scheme 4. Briefly, we anticipated that the 2,3-dialkyl naphthalene fluorophore of **19** would undergo fluorescence quenching in the presence of certain metal ions due to the heavy-metal effect and/or paramagnetic quenching induced by the binding of the metal ions at the ureidyl $\text{C}=\text{O}$ portals of **19**. Finally, we expected that addition of a competing guest that occupies the ureidyl $\text{C}=\text{O}$ portals and the hydrophobic cavity of **19** would force the release of the metal ion and result in an increase in the fluorescence

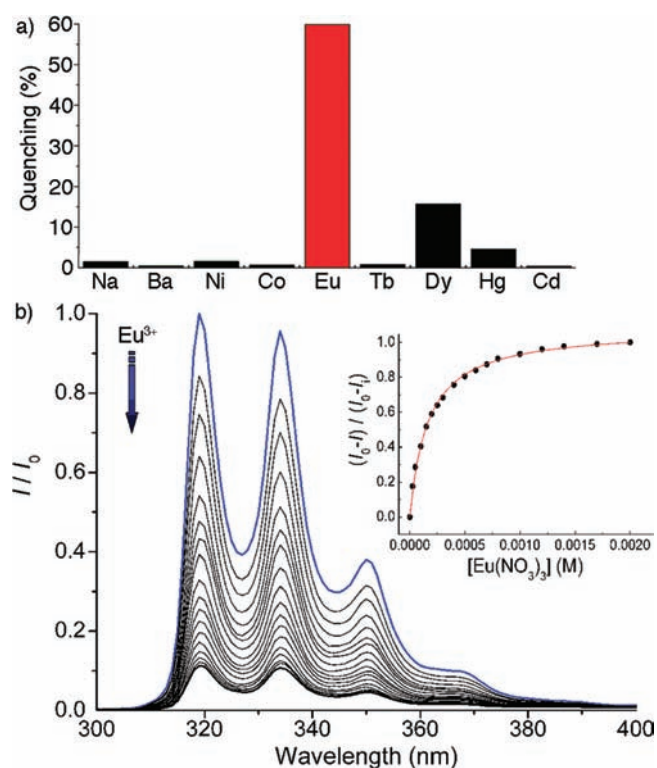


Figure 9. (a) Fluorescence quenching at 319 nm of **19** ($3 \mu\text{M}$) by various metal ions ($300 \mu\text{M}$). The measurements were carried out in water at pH 7, $\lambda_{\text{ex}} = 266 \text{ nm}$. (b) Fluorescence spectra of **19** ($3 \mu\text{M}$) upon the addition of an incremental amounts of Eu^{3+} in water at pH 7. $\lambda_{\text{ex}} = 266 \text{ nm}$. Inset: Normalized titration isotherm corresponding to the Eu^{3+} -induced quenching process.

intensity that would signal the presence and concentration of competing guest.

The Quencher. First, we investigated the ability of a variety of metal ions to quench the fluorescence of **19**. Figure 9a shows the percent quenching observed when **19** ($3 \mu\text{M}$) was treated individually with $300 \mu\text{M}$ of nine different metal ions. We chose these metal ions because they form stable hydrated ions at pH 7. Qualitatively it is easy to see that only Eu^{3+} and Dy^{3+} exhibit significant amounts of fluorescence quenching. We believe that Eu^{3+} coordinates to the ureidyl $\text{C}=\text{O}$ portals of **19** and quenches the naphthalene fluorescence by an intra-complex resonance energy transfer from naphthalene to Eu^{3+} . We selected Eu^{3+} which is able to quench approximately 60% of naphthalene fluorescence under these conditions for our further studies. First, we observed the changes in the fluorescence spectrum as a solution of **19** was titrated with Eu^{3+} (Figure 9b). The inset to Figure 9b shows the nonlinear least-squares best fit of the data to a standard 1:1 binding model with $K_a = 6.16 \times 10^3 \text{ M}^{-1}$. The magnitude of this K_a value dictates that we must use Eu^{3+} at concentrations at or above a concentration of $1/K_a$ ($1/6160 \text{ M}^{-1} = 162 \mu\text{M}$) for efficient quenching in the competition experiments described below.

*Use of the Ensemble Comprising **19** and Eu^{3+} To Sense **20** and the Biogenic Amine Histamine (**34**).* We next decided to explore the use of the ensemble comprising **19** and Eu^{3+} as a chemical sensor that exhibits a turn-on fluorescence response. For this purpose, we selected **20** as a prototypical guest for $\text{CB}[n]$ -type receptors, and histamine **34** which is a biogenic amine that is

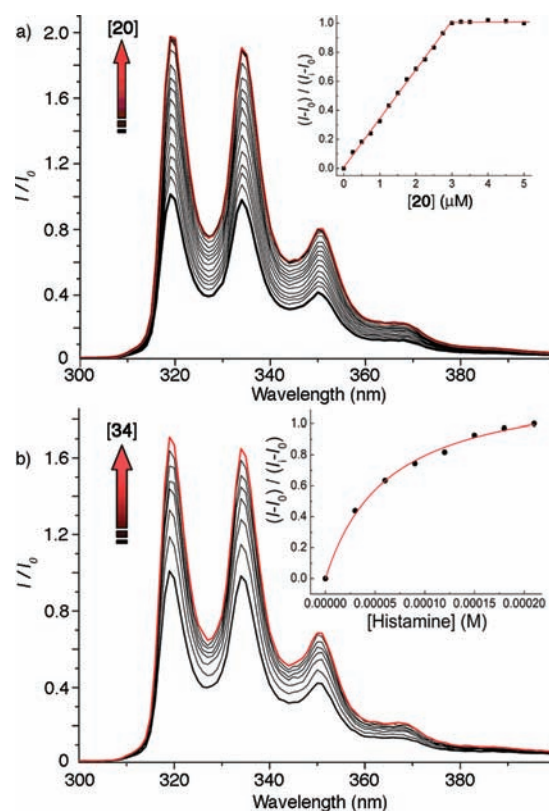


Figure 10. Fluorescence spectra of **19** ($3 \mu\text{M}$) and Eu^{3+} ($300 \mu\text{M}$) in water (pH 7) upon addition of incremental amounts of: (a) **20** and (b) **34**. $\lambda_{\text{ex}} = 266 \text{ nm}$. Insets: Normalized titration isotherm corresponding to the amine-induced fluorescence recovery.

involved in a variety of biological processes. For example, **34** triggers the inflammatory response, plays an important role in the immune response to pathogens, regulates physiological function in the gut, and acts as a neurotransmitter.⁵⁰ Figure 10a shows the fluorescence spectra recorded for a mixture of **19** and Eu^{3+} upon titration with a solution of **20**. As expected based on the design shown in Scheme 4, we observe an increase in fluorescence intensity which is consistent with **20** acting as a competitor for Eu^{3+} binding toward **19** which results in the formation of $\text{19} \cdot \text{20}$. The analysis of the fluorescence data is shown in the inset to Figure 10a which shows a breakpoint type-titration at $3 \mu\text{M}$ concentration which corresponds to the 1:1 $\text{19} \cdot \text{20}$ complex. Because the titration at this concentration of **19** ($3 \mu\text{M}$) consists of essentially two linear segments, it is not possible to fit this curve to obtain a K_a value for the $\text{19} \cdot \text{20}$ complex under these conditions. Figure 10b shows the fluorescence spectra obtained when a solution of **19** ($3 \mu\text{M}$) and Eu^{3+} ($300 \mu\text{M}$) was titrated with **34**. Similar to the observation for **20**, the fluorescence intensity increases as **34** competes with Eu^{3+} for binding to the ureidyl $\text{C}=\text{O}$ portals of **19**. We feel that the observation of significant fluorescence recovery in the case of **34**, which is a monoammonium ion, is significant. Monoammonium **34** occupies the hydrophobic cavity (Supporting Information Figure S35) and at least one ureidyl $\text{C}=\text{O}$ portal of **19** which might leave the other ureidyl $\text{C}=\text{O}$ portal available for binding to Eu^{3+} . The observation of the significant fluorescence recovery means that ammonium ions with a sufficiently large alkyl or aryl residue is sufficient to sterically block the other ureidyl $\text{C}=\text{O}$ portal from

Eu³⁺ binding. The inset to Figure 10b shows the best nonlinear fitting of the fluorescence intensity as a function of [34] to a 1:1 binding model with $K_a = 1.66 \times 10^4 \text{ M}^{-1}$. The present system responds to 34 in the 20–200 μM range, in accord with the measured K_a value for 19·34. We expect that this system, based on the highly selective host 19 and its moderate affinity toward 34, has significant potential for use in sensor development especially as a component of sensor arrays.

CONCLUSIONS

In summary, we have reported that the CB[*n*] forming reaction conducted between glycoluril (1) and less than 2 equiv of formaldehyde in the presence of *p*-xylylenediammonium ion (11) as template have a reduced tendency to undergo irreversible formation of CB[*n*] products which enables the straightforward isolation of 6C and bis-ns-CB[10] in multigram quantities. Template 11 influences the reaction by both kinetic and thermodynamic means: (1) by thermodynamically stabilizing 6C and bis-ns-CB[10] by host–guest binding, (2) by slowing down the rate of transformation of 6C into CB[6], and (3) by causing precipitation of the 6C·11 complex. Hexamer 6C can be transformed into monofunctionalized CB[6] derivatives 13, 16, 17, and 19 in very good yields on gram scale without the need for chromatographic purification. Host 13, but not 16, 17, or 19, undergoes self-association processes which highlights the need to be vigilant in the molecular design of CB[6] derivatives for advanced applications. We studied the 19·guest complexes by ¹H NMR methods and observed that the recognition properties of 19 are comparable to those of CB[6] in terms of slow exchange kinetics on the NMR time scale and values of K_a . Finally, we demonstrated that 19, with its covalently attached naphthalene chromophore and its ureidyl C=O portals and hydrophobic cavity binding sites, undergoes fluorescence quenching in the presence of Eu³⁺ which forms the basis for fluorescence turn-on assays for suitable CB[*n*] guests like 20 and histamine 34.

We believe the results of this paper have implications that will strongly impact the future development of the synthesis and applications of functionalized CB[*n*] molecular containers. First, the ready availability of 6C on gram scale and its high yielding transformation into monofunctionalized CB[6] derivatives will allow their incorporation into more complex solution or surface bound architectures for advanced technological or biomimetic applications. Second, the demonstration that both the CB[*n*] forming reaction and the macrocyclization of glycoluril oligomer 6C with phthalaldehydes is subject to template effects delivers an unprecedented level of control over the formation of CB[*n*]-type receptors. For example, it is straightforward to predict that the use of larger templates might deliver the currently unknown glycoluril heptamer 7C and octamer 8C as building blocks for CB[7] or CB[8] derivatives and that chiral templates may lead to chiral and enantiomerically pure CB[*n*]-type receptors for chiral recognition. Third, the demonstration of 11 and derivatives as a diagnostic probe for ¹H NMR monitoring of CB[*n*]-type reactions promises to impact all synthetic studies in the CB[*n*] area. Finally, the ability to prepare monofunctionalized CB[*n*] derivatives tailor-made with reactive functional groups (e.g., NO₂, CO₂H) or synergistic structural elements (e.g., fluorophores) has the potential to enlarge the utility of CB[*n*]-type receptors as components of more complex systems including sensor arrays and for fluorescence imaging applications.

ASSOCIATED CONTENT

S Supporting Information. Synthetic procedures and characterization data for all new compounds, ¹H NMR spectra for selected host–guest complexes, ¹H NMR dilution experiments, NMR spectra used in binding constant determination, and procedures used to monitor the templated reactions. This material is available free of charge via the Internet at <http://pubs.acs.org>.

AUTHOR INFORMATION

Corresponding Author

LIsaacs@umd.edu; pavel@bgsu.edu

ACKNOWLEDGMENT

We thank the National Science Foundation (CHE-0615049 and CHE-1110911 to L.L., and CHE-0750303 and EXP-LA 0731153 to P.A.) for financial support. D.L. and J.B.W. thank the Department of Education for GAANN fellowships (P200A090105).

REFERENCES

- (1) Behrend, R.; Meyer, E.; Rusche, F. *Liebigs Ann. Chem.* **1905**, 339, 1–37. Freeman, W. A.; Mock, W. L.; Shih, N.-Y. *J. Am. Chem. Soc.* **1981**, *103*, 7367–7368. Kim, J.; Jung, I.-S.; Kim, S.-Y.; Lee, E.; Kang, J.-K.; Sakamoto, S.; Yamaguchi, K.; Kim, K. *J. Am. Chem. Soc.* **2000**, *122*, 540–541. Day, A. I.; Blanch, R. J.; Arnold, A. P.; Lorenzo, S.; Lewis, G. R.; Dance, I. *Angew. Chem., Int. Ed.* **2002**, *41*, 275–277. Liu, S.; Zavalij, P. Y.; Isaacs, L. *J. Am. Chem. Soc.* **2005**, *127*, 16798–16799.
- (2) Day, A. I.; Arnold, A. P.; Blanch, R. J.; Snushall, B. *J. Org. Chem.* **2001**, *66*, 8094–8100.
- (3) Lee, J. W.; Samal, S.; Selvapalam, N.; Kim, H.-J.; Kim, K. *Acc. Chem. Res.* **2003**, *36*, 621–630. Lagona, J.; Mukhopadhyay, P.; Chakrabarti, S.; Isaacs, L. *Angew. Chem., Int. Ed.* **2005**, *44*, 4844–4870.
- (4) Mock, W. L.; Shih, N. Y. *J. Org. Chem.* **1986**, *51*, 4440–4446.
- (5) Liu, S.; Ruspic, C.; Mukhopadhyay, P.; Chakrabarti, S.; Zavalij, P. Y.; Isaacs, L. *J. Am. Chem. Soc.* **2005**, *127*, 15959–15967.
- (6) Rekharsky, M. V.; Mori, T.; Yang, C.; Ko, Y. H.; Selvapalam, N.; Kim, H.; Sobransingh, D.; Kaifer, A. E.; Liu, S.; Isaacs, L.; Chen, W.; Moghaddam, S.; Gilson, M. K.; Kim, K.; Inoue, Y. *Proc. Natl. Acad. Sci. U.S.A.* **2007**, *104*, 20737–20742. Kaifer, A. E.; Li, W.; Yi, S. *Isr. J. Chem.* **2011**, *51*, 496–505.
- (7) Nau, W. M.; Florea, M.; Assaf, K. I. *Isr. J. Chem.* **2011**, *51*, 559–577.
- (8) Ko, Y. H.; Kim, E.; Hwang, I.; Kim, K. *Chem. Commun.* **2007**, 1305–1315.
- (9) Meschke, C.; Buschmann, H.-J.; Schollmeyer, E. *Polymer* **1998**, *40*, 945–949. Tuncel, D.; Steinke, J. H. G. *Chem. Commun.* **1999**, 1509–1510. Ling, Y.; Kaifer, A. E. *Chem. Mater.* **2006**, *18*, 5944–5949. Choi, S. W.; Ritter, H. *Macromol. Rapid Commun.* **2007**, *28*, 101–108. Liu, Y.; Ke, C.-F.; Zhang, H.-Y.; Wu, W.-J.; Shi, J. *J. Org. Chem.* **2007**, *72*, 280–283. Liu, Y.; Shi, J.; Chen, Y.; Ke, C.-F. *Angew. Chem., Int. Ed.* **2008**, *47*, 7293–7296. Nally, R.; Scherman, O. A.; Isaacs, L. *Supramol. Chem.* **2010**, *22*, 683–690. Das, D.; Scherman, O. A. *Isr. J. Chem.* **2011**, *51*, 489–490. Chen, Y.; Zhang, Y.-M.; Liu, Y. *Isr. J. Chem.* **2011**, *51*, 515–524.
- (10) Bush, M. E.; Bouley, N. D.; Urbach, A. R. *J. Am. Chem. Soc.* **2005**, *127*, 14511–14517. Praetorius, A.; Bailey, D. M.; Schwarzlose, T.; Nau, W. M. *Org. Lett.* **2008**, *10*, 4089–4092. Wu, J.; Isaacs, L. *Chem.—Eur. J.* **2009**, *15*, 11675–11680. Biedermann, F.; Rauwald, U.; Cziferszky, M.; Williams, K. A.; Gann, L. D.; Guo, B. Y.; Urbach, A. R.; Bielawski, C. W.; Scherman, O. A. *Chem.—Eur. J.* **2010**, *16*, 13716–13722. Ghale, G.; Ramalingam, V.; Urbach, A. R.; Nau, W. M. *J. Am. Chem. Soc.* **2011**, *133*, 7528–7535.

- (11) Hennig, A.; Bakirci, H.; Nau, W. M. *Nat. Methods* **2007**, *4*, 629–632.
- (12) Jeon, Y. J.; Kim, H.; Jon, S.; Selvapalam, N.; Oh, D. H.; Seo, I.; Park, C.-S.; Jung, S. R.; Koh, D.-S.; Kim, K. *J. Am. Chem. Soc.* **2004**, *126*, 15944–15945. Liu, S.; Zavalij, P. Y.; Lam, Y.-F.; Isaacs, L. *J. Am. Chem. Soc.* **2007**, *129*, 11232–11241. Liu, S.; Shukla, A. D.; Gadde, S.; Wagner, B. D.; Kaifer, A. E.; Isaacs, L. *Angew. Chem., Int. Ed.* **2008**, *47*, 2657–2660. Ghosh, S.; Isaacs, L. *J. Am. Chem. Soc.* **2010**, *132*, 4445–4454.
- (13) Huang, W.-H.; Zavalij, P. Y.; Isaacs, L. *Org. Lett.* **2009**, *11*, 3918–3921.
- (14) Isaacs, L. *Chem. Commun.* **2009**, 619–629.
- (15) Wheate, N. J.; Buck, D. P.; Day, A. I.; Collins, J. G. *Dalton Trans.* **2006**, 451–458. Saleh, N.; Koner, A. L.; Nau, W. M. *Angew. Chem., Int. Ed.* **2008**, *47*, 5398–5401. Hettiarachchi, G.; Nguyen, D.; Wu, J.; Lucas, D.; Ma, D.; Isaacs, L.; Briken, V. *PLoS One* **2010**, *5*, e10514. Kim, C.; Agasti, S. S.; Zhu, Z.; Isaacs, L.; Rotello, V. M. *Nat. Chem.* **2010**, *2*, 962–966. Uzunova, V. D.; Cullinane, C.; Brix, K.; Nau, W. M.; Day, A. I. *Org. Biomol. Chem.* **2010**, *8*, 2037–2042. Macartney, D. H. *Isr. J. Chem.* **2011**, *51*, 600–615. Walker, S.; Oun, R.; McInnes, F. J.; Wheate, N. J. *Isr. J. Chem.* **2011**, *51*, 616–624. Dong, N.; Xue, S.-F.; Zhu, Q.-J.; Tao, Z.; Zhao, Y.; Yang, L.-X. *Supramol. Chem.* **2008**, *20*, 659–665. Park, K. M.; Suh, K.; Jung, H.; Lee, D.-W.; Ahn, Y.; Kim, J.; Baek, K.; Kim, K. *Chem. Commun.* **2009**, 71–73.
- (16) Kim, E.; Kim, D.; Jung, H.; Lee, J.; Paul, S.; Selvapalam, N.; Yang, Y.; Lim, N.; Park, C. G.; Kim, K. *Angew. Chem., Int. Ed.* **2010**, *49*, 4405–4408. Park, K. M.; Lee, D.-W.; Sarkar, B.; Jung, H.; Kim, J.; Ko, Y. H.; Lee, K. E.; Jeon, H.; Kim, K. *Small* **2010**, *6*, 1430–1441.
- (17) Jeon, Y. J.; Kim, S.-Y.; Ko, Y. H.; Sakamoto, S.; Yamaguchi, K.; Kim, K. *Org. Biomol. Chem.* **2005**, *3*, 2122–2125.
- (18) Miyahara, Y.; Abe, K.; Inazu, T. *Angew. Chem., Int. Ed.* **2002**, *41*, 3020–3023. Day, A. I.; Arnold, A. P.; Blanch, R. J. (Unisearch Limited, Australia), U.S. Patent US 2003/0140787, 2003 [*Chem. Abstr.* **2003**, *139*, 135453]. Grechin, A. G.; Buschmann, H.-J.; Schollmeyer, E. *Angew. Chem., Int. Ed.* **2007**, *46*, 6499–6501. Fusaro, L.; Locci, E.; Lai, A.; Luhmer, M. J. *Phys. Chem. B* **2008**, *112*, 15014–15020. Lim, S.; Kim, H.; Selvapalam, N.; Kim, K.-J.; Cho, S. J.; Seo, G.; Kim, K. *Angew. Chem., Int. Ed.* **2008**, *47*, 3352–3355. Huber, G.; Legrand, F.-X.; Lewin, V.; Baumann, D.; Heck, M.-P.; Berthault, P. *ChemPhysChem* **2011**, *12*, 1053–1055. Kim, H.; Kim, Y.; Yoon, M.; Lim, S.; Park, S. M.; Seo, G.; Kim, K. *J. Am. Chem. Soc.* **2010**, *132*, 12200–12202.
- (19) Mock, W. L.; Irra, T. A.; Wepsiec, J. P.; Adhya, M. J. *Org. Chem.* **1989**, *54*, 5302–5308. Jon, S. Y.; Ko, Y. H.; Park, S. H.; Kim, H.-J.; Kim, K. *Chem. Commun.* **2001**, 1938–1939. Pattabiraman, M.; Natarajan, A.; Kaanumalle, L. S.; Ramamurthy, V. *Org. Lett.* **2005**, *7*, 529–532. Wang, R.; Yuan, L.; Macartney, D. H. *J. Org. Chem.* **2006**, *71*, 1237–1239. Kloeck, C.; Dsouza, R. N.; Nau, W. M. *Org. Lett.* **2009**, *11*, 2595–2598. Basilio, N.; Garcia-Rio, L.; Moreira, J. A.; Pessego, M. J. *Org. Chem.* **2010**, *75*, 848–855. Lu, X.; Masson, E. *Org. Lett.* **2010**, *12*, 2310–2313. Pemberton, B. C.; Singh, R. K.; Johnson, A. C.; Jockusch, S.; Da Silva, J. P.; Ugrinov, A.; Turro, N. J.; Srivastava, D. K.; Sivaguru, J. *Chem. Commun.* **2011**, *47*, 6323–6325. Tuncel, D.; Uenal, O.; Artar, M. *Isr. J. Chem.* **2011**, *51*, 525–532.
- (20) Jon, S. Y.; Selvapalam, N.; Oh, D. H.; Kang, J.-K.; Kim, S.-Y.; Jeon, Y. J.; Lee, J. W.; Kim, K. *J. Am. Chem. Soc.* **2003**, *125*, 10186–10187. Kim, K.; Selvapalam, N.; Ko, Y. H.; Park, K. M.; Kim, D.; Kim, J. *Chem. Soc. Rev.* **2007**, *36*, 267–279.
- (21) Ko, Y. H.; Hwang, I.; Lee, D.-W.; Kim, K. *Isr. J. Chem.* **2011**, *51*, 506–514. Lee, D.-W.; Park, K. M.; Banerjee, M.; Ha, S. H.; Lee, T.; Suh, K.; Paul, S.; Jung, H.; Kim, J.; Selvapalam, N.; Ryu, S. H.; Kim, K. *Nat. Chem.* **2011**, *3*, 154–159. Munteanu, M.; Choi, S.; Ritter, H. *Macromolecules* **2009**, *42*, 3887–3891.
- (22) Isaacs, L. *Isr. J. Chem.* **2011**, *51*, 578–591.
- (23) Lagona, J.; Fettinger, J. C.; Isaacs, L. *Org. Lett.* **2003**, *5*, 3745–3747. Lagona, J.; Fettinger, J. C.; Isaacs, L. *J. Org. Chem.* **2005**, *70*, 10381–10392. Wagner, B. D.; Boland, P. G.; Lagona, J.; Isaacs, L. *J. Phys. Chem. B* **2005**, *109*, 7686–7691.
- (24) Isaacs, L.; Park, S.-K.; Liu, S.; Ko, Y. H.; Selvapalam, N.; Kim, Y.; Kim, H.; Zavalij, P. Y.; Kim, G.-H.; Lee, H.-S.; Kim, K. *J. Am. Chem. Soc.* **2005**, *127*, 18000–18001. Liu, S.; Kim, K.; Isaacs, L. *J. Org. Chem.* **2007**, *72*, 6840–6847.
- (25) (a) Huang, W.-H.; Liu, S.; Zavalij, P. Y.; Isaacs, L. *J. Am. Chem. Soc.* **2006**, *128*, 14744–14745. (b) Huang, W.-H.; Zavalij, P. Y.; Isaacs, L. *Org. Lett.* **2008**, *10*, 2577–2580. (c) Nally, R.; Isaacs, L. *Tetrahedron* **2009**, *65*, 7249–7258. (d) Wittenberg, J. B.; Costales, M. G.; Zavalij, P. Y.; Isaacs, L. *Chem. Commun.* **2011**, *47*, 9420–9422.
- (26) Huang, W.-H.; Zavalij, P. Y.; Isaacs, L. *Angew. Chem., Int. Ed.* **2007**, *46*, 7425–7427.
- (27) Huang, W.-H.; Zavalij, P. Y.; Isaacs, L. *J. Am. Chem. Soc.* **2008**, *130*, 8446–8454.
- (28) Stancl, M.; Svec, J.; Sindelar, V. *Isr. J. Chem.* **2011**, *51*, 592–599.
- (29) Chakraborty, A.; Wu, A.; Witt, D.; Lagona, J.; Fettinger, J. C.; Isaacs, L. *J. Am. Chem. Soc.* **2002**, *124*, 8297–8306.
- (30) Lucas, D.; Isaacs, L. *Org. Lett.* **2011**, *13*, 4112–4115.
- (31) Day, A. I.; Arnold, A. P.; Blanch, R. J. (Unisearch Limited, Australia), PCT Int. Appl. WO 2000068232, 2000 [*Chem. Abstr.* **2000**, *133*, 362775]. Blanch, R. J.; Sleeman, A. J.; White, T. J.; Arnold, A. P.; Day, A. I. *Nano Lett.* **2002**, *2*, 147–149. Day, A. I.; Blanch, R. J.; Coe, A.; Arnold, A. P. *J. Inclusion Phenom. Macrocyclic Chem.* **2002**, *43*, 247–250.
- (32) Ma, D.; Gargulakova, Z.; Zavalij, P. Y.; Sindelar, V.; Isaacs, L. *J. Org. Chem.* **2010**, *75*, 2934–2941.
- (33) Anderson, S.; Anderson, H. L.; Sanders, J. K. M. *Acc. Chem. Res.* **1993**, *26*, 469–475.
- (34) We have conducted the reaction to form **6C** successfully at temperatures ranging from 50 to 60 °C. At 50 °C, precipitation is observed after 7 days. We prefer to use 58 °C to decrease the time required to complete the reaction while minimizing the irreversible transformation to CB[n].
- (35) The reaction that forms **6C** and bis-ns-CB[10] is heterogeneous during the initial stages of the reaction. We believe that the size and nature of the reaction vessel influence the outcome of the reaction because of differences that occur during the initial mixing of the solid reactants with the HCl solvent. The solubility of various CB[n] compounds are known to depend sensitively on [HCl]. Accordingly, the nature of the vessel closure may influence the outcome of the reaction by preventing escape of HCl during the reaction.
- (36) It may seem counterintuitive to wash the reaction mixture with H₂O given the known poor solubility of CB[6]. We believe that the presence of **11** and HCl in the crude solid increase the solubility of CB[6] which makes the washing procedure effective.
- (37) The MMFF minimized geometry of **6C**·**11** shown in Figure 2 is not unique. When minimizations are performed from different starting geometries of **6C**·**11**, different minima are obtained which differ in particular with respect to the orientation of the CH₂NH₃⁺ groups relative to the mean plane of the aromatic ring. In all cases, however, the reactive NH tips of **6C** are still held apart.
- (38) Haris, S. P.; Zhang, Y.; Le Bourdonnec, B.; McCurdy, C. R.; Portoghese, P. S. *J. Med. Chem.* **2007**, *50*, 3392–3396.
- (39) Zhu, P. C.; Wang, D.-H.; Lu, K.; Mani, N. *Sci. China, Ser. B: Chem.* **2007**, *50*, 249–252.
- (40) The condensation reactions between **6C** and the phthaldehydes are relatively clean and consist predominantly of starting hexamer, the desired CB[6] derivative, and the chiral intermediate (e.g., Figure 7). The lower isolated yield reflects the challenges inherent in purification of the reaction mixtures.
- (41) Miao, Q.; Lefenfeld, M.; Nguyen, T.-Q.; Siegrist, T.; Kloc, C.; Nuckolls, C. *Adv. Mater.* **2005**, *17*, 407–412.
- (42) Zhao, Y.; Xue, S.; Zhu, Q.; Tao, Z.; Zhang, J.; Wei, Z.; Long, L.; Hu, M.; Xiao, H.; Day, A. I. *Chin. Sci. Bull.* **2004**, *49*, 1111–1116.
- (43) Samsonenko, D. G.; Virovets, A. V.; Lipkowsky, J.; Gerasko, O. A.; Fedin, V. P. *J. Struct. Chem.* **2002**, *43*, 664–668. Huang, W. H.; Zavalij, P. Y.; Isaacs, L. *Acta Crystallogr., Sect. E: Struct. Rep. Online* **2007**, *E63*, o1060–o1062.
- (44) We have previously observed a CB[n]-type product with an NCOCN-bridge during the reaction between nor-seco-CB[6] and **12**. See ref 25b.

(45) Two diastereomers are consistent with the ESI–MS and NMR data. Both feature top-bottom connections between N-atoms at the termini of the hexamer unit of (\pm)-**21** and both feature NCOCN-bridges, but differ in the chirality of the two newly formed stereogenic centers. The singlet observed at 6.59 ppm which corresponds to the N(CH)O(CH)N protons signifies that these two protons are equivalent and homotopic. The Supporting Information depicts an MMFF minimized structures of both diastereomers for comparison.

(46) For an example of a template effect in bambusuril chemistry, see: Havel, V.; Svec, J.; Wimmerova, M.; Dusek, M.; Pojarova, M.; Sindelar, V. *Org. Lett.* **2011**, *13*, 4000–4003.

(47) Chinai, J. M.; Taylor, A. B.; Ryno, L. M.; Hargreaves, N. D.; Morris, C. A.; Hart, P. J.; Urbach, A. R. *J. Am. Chem. Soc.* **2011**, *133*, 8810–8813. Urbach, A. R.; Ramalingam, V. *Isr. J. Chem.* **2011**, *51*, 664–678.

(48) Anslyn, E. V. *J. Org. Chem.* **2007**, *72*, 687–699.

(49) Buschmann, H. J.; Cleve, E.; Schollmeyer, E. *Inorg. Chim. Acta* **1992**, *193*, 93–97. Jeon, Y.-M.; Kim, J.; Whang, D.; Kim, K. *J. Am. Chem. Soc.* **1996**, *118*, 9790–9791. Gerasko, O. A.; Sokolov, M. N.; Fedin, V. P. *Pure Appl. Chem.* **2004**, *76*, 1633–1646.

(50) *Biomedical Aspects of Histamine: Current Perspectives*; Shahid, M., Khardori, N., Khan, R. A., Tripathi, T., Eds.; Springer: New York, 2010; *Histamine: Biology and Medical Aspects*; Falus, A., Ed.; S. Karger AG: Basel; 2004.